

UC Davis

UC Davis Previously Published Works

Title

Microtubule +TIPs in Aspergillus

Permalink

<https://escholarship.org/uc/item/6k8097jx>

Journal

Molecular Microbiology, 94(3)

ISSN

0950-382X

Authors

Zeng, Cui J Tracy

Kim, Hye-Ryun

Arispuro, Irasema Vargas

et al.

Publication Date

2014-11-01

DOI

10.1111/mmi.12792

Peer reviewed

Microtubule plus end-tracking proteins play critical roles in directional growth of hyphae by regulating the dynamics of cytoplasmic microtubules in *Aspergillus nidulans*

Cui J. Tracy Zeng,¹ Hye-Ryun Kim,^{1†}
Irasema Vargas Arispuro,² Jung-Mi Kim,^{1‡}
An-Chi Huang¹ and Bo Liu^{1*}

¹Department of Plant Biology, University of California, Davis, CA 95616, USA.

²Centro de Investigación en Alimentación y Desarrollo, A.C., Carr. a la Victoria Km 0.6 83304 Hermosillo, Sonora, Mexico.

Summary

Cytoplasmic microtubules (MTs) serve as a rate-limiting factor for hyphal tip growth in the filamentous fungus *Aspergillus nidulans*. We hypothesized that this function depended on the MT plus end-tracking proteins (+TIPs) including the EB1 family protein EBA that decorated the MT plus ends undergoing polymerization. The *ebaΔ* mutation reduced colony growth and the mutant hyphae appeared in an undulating pattern instead of exhibiting unidirectional growth in the control. These phenotypes were enhanced by a mutation in another +TIP gene *clipA*. EBA was required for plus end-tracking of CLIPA, the Kinesin-7 motor KipA, and the XMAP215 homologue AlpA. In addition, cytoplasmic dynein also depended on EBA to track on most polymerizing MT plus ends, but not for its conspicuous appearance at the MT ends near the hyphal apex. The loss of EBA reduced the number of cytoplasmic MTs and prolonged dwelling times for MTs after reaching the hyphal apex. Finally, we found that colonies were formed in the absence of EBA, CLIPA, and NUDA together, suggesting that they were dispensable for fundamental functions of MTs. This study provided a comprehensive delineation of the relationship among different +TIPs and their contributions to MT

dynamics and unidirectional hyphal expansion in filamentous fungi.

Introduction

In filamentous fungi, vegetative growth is largely dependent on robust expansion at the apex of the hyphal tip cells. The actin cytoskeleton plays pivotal roles in organizing vesicles at the apex and driving robust exocytosis and endocytosis associated with tip growth in *Aspergillus nidulans* and other fungi (Harris *et al.*, 2005). Conversely, microtubules (MTs) serve as tracks for long distance transport of vesicles towards the hyphal tip region as demonstrated in *A. nidulans* (Horio and Oakley, 2005). In addition, MTs likely influence the activities of the actin microfilaments near the hyphal apex (Fischer *et al.*, 2008).

In filamentous fungi like *A. nidulans*, MTs are nucleated primarily at the MT-organizing centre, the spindle pole body (SPB), where the MT minus ends are often anchored (Xiang and Oakley, 2010). In apical cells of growing hyphae, cytoplasmic MTs rapidly polymerize towards the hyphal apex and depolymerize when the plus ends encounter the plasma membrane or other barriers (Han *et al.*, 2001). The polymerizing MT plus ends explore the cytoplasm and consequently establish interactions with other proteins that may be important for tip growth. Furthermore, these MTs are critical for delivering materials required for tip growth and maintaining the integrity of the tip growth machinery that involves the actin microfilaments (Horio, 2007; Fischer *et al.*, 2008). In *A. nidulans*, the hyphal apical cell bears a growth rate of several micrometre per minute, much faster than that in unicellular fungi yeasts (Riquelme *et al.*, 2003; Horio and Oakley, 2005; Horio, 2007). The fact that the growth slows down drastically upon benomyl-induced MT depolymerization suggests that cytoplasmic MTs serve as a critical rate-limiting factor during tip growth (Oakley and Morris, 1980; Horio and Oakley, 2005). Because MT polymerization rates among yeasts and filamentous fungi are similar in the range of ~ 5–10 $\mu\text{m min}^{-1}$ (Horio and Oakley, 2005; Grallert *et al.*, 2006), it is unclear how cytoplasmic MTs assist hyphal apical cells to achieve such a remarkable growth rate.

Accepted 7 September, 2014. *For correspondence. E-mail bliu@ucdavis.edu; Tel. (+1) 530 754 8138; Fax (+1) 530 752 5410. †Present address: Department of Biomedical Science, CHA University, Gyeonggi-do, Seoul 135-081, Korea. ‡Present address: Department of Bio-Environmental Chemistry, Wonkwang University, 460 Iksan-Daero, Iksan, Jeonbuk, 570-749, Korea. The authors have no conflicts of interest in this study.

Among MT-associated proteins (MAPs) that regulate MT dynamics, many structurally unrelated proteins specifically act at MT plus ends and are collectively called MT plus end-tracking proteins or +TIPs (Galjart, 2010; Jiang and Akhmanova, 2011; Mimori-Kiyosue, 2011). Most of these proteins dissociate from MT plus ends when polymerization ceases or when MTs undergo depolymerization. The central figure of +TIPs is an approximately 250- to 300-amino-acid protein called end-binding 1 (EB1) which was first isolated as a binding partner of the C-terminus of the tumour suppressor protein adenomatous polyposis coli (APC) (Su *et al.*, 1995). EB1 family proteins form homodimers and contain a calponin homology (CH) and an EB1 homology (EBH) domains (Akhmanova and Steinmetz, 2010). Functions of EB1 vary among tested systems, ranging from promoting MT growth rates to increasing MT catastrophe frequencies (Tirnauer *et al.*, 2002; Busch and Brunner, 2004; Komarova *et al.*, 2009). Different scenarios likely arise from different patterns of protein interaction involving EB1 at MT plus ends in different cells (Galjart, 2010; Mimori-Kiyosue, 2011). In metazoans, EB1 is absolutely essential for organizing MTs into characteristic arrays in both interphase and mitosis (Tirnauer and Bierer, 2000; Rogers *et al.*, 2002). In contrast, fungi like yeasts retain relatively robust growth and their cells continue to divide upon the deletion of single genes encoding EB1 homologues (Schwartz *et al.*, 1997; Busch and Brunner, 2004). Thus one would assume that other proteins may act in concert with EB1 to regulate the dynamics of MT plus ends in these fungi. Since the discovery of MT plus end-tracking phenomenon exhibited by the founding member of +TIPs, CLIP170, the list of such proteins has been growing and most of them can directly bind/interact with MTs (Mimori-Kiyosue, 2011). Extensive investigations have reached the consensus that EB1 is essential for other +TIPs to track at MT plus ends through direct interaction with EB1 (Akhmanova and Steinmetz, 2010). However, diverse and specified functions often are associated with +TIPs other than EB1 (Mimori-Kiyosue, 2011).

It is unclear how the behaviour of MT plus ends would influence rapid tip growth in hyphal apical cells. A number of +TIPs have been identified in *A. nidulans*. Examples include the cytoplasmic dynein motor complex and its regulators like dynactin (Xiang *et al.*, 2000; Han *et al.*, 2001; Zhang *et al.*, 2003). Dynein is the primary motor for nuclear migration in growing hyphae (Xiang *et al.*, 1994). However, it is unclear whether the plus end-tracking activity is associated with the motor's function in nuclear migration. The CLIPA protein, despite being distantly related to the CLIP170 family proteins of animal origins, also exhibits prominent MT plus end-tracking localization (Efimov *et al.*, 2006). Although the deletion of the *clipA* gene leads to a reduction in the catastrophe rate of cytoplasmic MTs when they reach the hyphal apex, the null mutant does

not show noticeable phenotypes in colony formation and conidiation when compared to the wild-type control (Efimov *et al.*, 2006). Besides dynein and CLIPA, the Kinesin-7 motor KipA also tracks at polymerizing MT plus ends in tip cells and is required for cytoplasmic MTs to converge near the apex (Konzack *et al.*, 2005). In the *kipA* null mutant, hyphal apical cells often lose the directionality in polar growth and highly curved hyphae are produced. Interestingly, the XMAP215 family protein AlpA decorates both MT plus ends and the spindle pole body and mutants lacking the protein produce highly curved hyphae as well (Enke *et al.*, 2007). In *A. nidulans*, highly curved hyphae can also be produced when the fungus is challenged by MT-depolymerizing agents like benomyl (Sampson and Heath, 2005). Obviously, this terminal growth phenotype can be caused by more than just destabilization of cytoplasmic MTs. It is intriguing how the loss of one or more +TIPs could alter the dynamic behaviour of cytoplasmic MTs and consequently tip growth of apical cells.

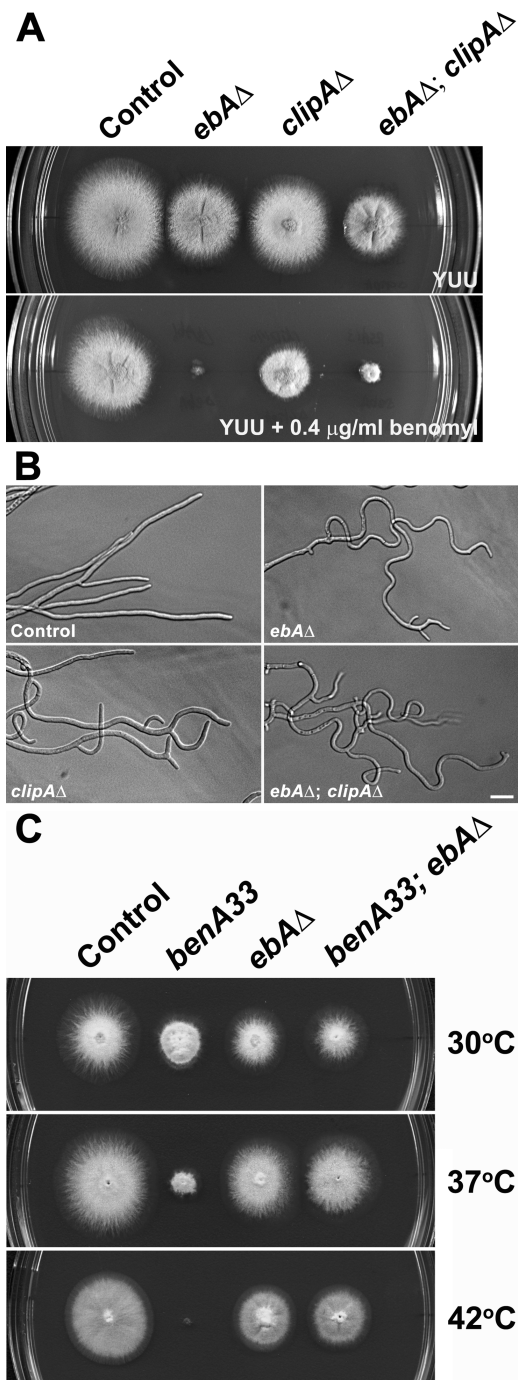
The EB1's MT-tracking activity has been reconstituted *in vitro* using purified recombinant protein (Bieling *et al.*, 2007). Further *in vitro* assays were aimed at dissecting how different +TIPs might interact at MT plus ends and influence each other's function (Dixit *et al.*, 2009; Skube *et al.*, 2010). In actively growing cells, however, polymerizing MT plus ends encounter a complicated network of proteins that interact with each other. It is puzzling how a large number of proteins and protein complexes are able to interact, often simultaneously, with plus ends of cytoplasmic MTs *in vivo*. To understand vegetative growth in filamentous fungi, we wished to integrate functions of different +TIPs with the growth behaviour of hyphal apical cells. *A. nidulans* offers us a convenient and informative *in vivo* system to investigate how functions of +TIPs are harnessed to aid the rapid expansion of hyphal apices.

In this report, we found that the EB1 family protein EBA regulated the dynamics of MT plus ends and played a critical role in hyphal tip growth in *A. nidulans*. This genetically tractable system also allowed us to conclude that EBA was required for other +TIPs to track at MT plus ends. But the functions of these non-EBA +TIPs were not absolutely dependent on their MT plus end-tracking activity. Surprisingly, it was found that in the absence of three critical +TIPs, EBA, CLIPA, and cytoplasmic dynein, hyphal tip cells were able to undergo reasonable polar growth and the mutant was able to form colonies although their growth was significantly retarded.

Results

EBA is an MT-stabilizing factor required for hyphal apical cells to maintain unidirectional growth

The EB1 proteins are essential for MT organization during interphase and mitosis in animal cells (Rogers *et al.*,



2002). In *A. nidulans*, the EB1 orthologue EBA is encoded by the AN2862 locus. We tested whether the null *ebA*Δ mutation would cause obvious growth defects in *A. nidulans*. Similar to the *clipA*Δ null mutant (Efimov *et al.*, 2006), the *ebA*Δ mutant formed conidiating colonies with reduced sizes (Fig. 1A). The reduction of colony growth in *ebA*Δ was more obvious than that caused by the *clipA*Δ mutation. To take one step further, it was also tested whether the absence of the EBA protein would affect the stability of

Fig. 1. Growth phenotypes resulted from the *ebA*Δ mutation.

A. Colony formation by the control (R153), *ebA*Δ (LBA66), *clipA*Δ, and *ebA*Δ; *clipA*Δ double mutant (RSA13) on rich (YUU) and benomyl media. The *ebA*Δ mutation causes hypersensitivity to benomyl.
B. Directional extension of hyphae is replaced by wavy growth patterns in the *ebA*Δ and *clipA*Δ mutants. Enhanced growth defects were observed in the *ebA*Δ; *clipA*Δ double mutant. Scale bar, 10 µm.
C. The *ebA*Δ mutation suppresses the MT hyperstabilization phenotype caused by the *benA33* mutation. At the restrictive temperature of 42°C, *benA33* (RSA197) alone prevented colony formation. The *benA33*; *ebA*Δ double mutant (RSA75) forms colonies indistinguishable from those of the *ebA*Δ mutant.

cytoplasmic MTs. When conidia were inoculated on media containing the MT-depolymerizing agent benomyl at 0.4 µg ml⁻¹ which did not cause a significant growth defect in the control strain, the *ebA*Δ strain failed to form a viable colony, indicating that the mutant was hypersensitive to the drug (Fig. 1A). In contrast, the *clipA*Δ mutant formed a conidiating colony albeit being smaller than that of the control. Because null mutations of orthologues of the *ebA* and *clipA* genes often render synthetic lethality in unicellular yeasts (Schwartz *et al.*, 1997), we tested whether a similar phenotype could be observed by creating the *ebA*Δ; *clipA*Δ double mutant. The double mutant formed colonies that were smaller than the *ebA*Δ single mutant and the colonies produced conidia (Fig. 1A). Surprisingly, it even formed small but viable colonies in the presence of 0.4 µg ml⁻¹ benomyl (Fig. 1A). Thus, in *A. nidulans* fundamental functions of MTs do not require the contributions from EBA and CLIPA.

Normally, hyphal tip cells produced by young colonies of the control strain exhibited robust and sustained unidirectional growth so that the hyphae more or less exhibited linear and straight appearances (Fig. 1B). The *ebA*Δ tip cells, however, showed highly wavy or curved patterns (Fig. 1B). Wavy hyphae were also formed by the apical cells of the *clipA*Δ mutant, although to a lesser extent (Fig. 1B). A similar growth phenotype has been reported for the null mutant of *kipA* encoding a kinesin motor acting at MT plus ends (Konzack *et al.*, 2005). The wavy hyphal growth phenotype was more obvious when both *ebA* and *clipA* were knocked out (Fig. 1B). Because the application of low doses of MT-depolymerizing agent also causes hyphal tip cells to grow in a curved pattern (Horio and Oakley, 2005), these results suggest that EBA contributes to stabilizing MTs in hyphal cells.

The results summarized above suggested that MTs might have become more labile in the absence of EBA. To test this hypothesis, we employed the *benA33* mutation in a β-tubulin gene, which causes an MT hyper-stabilization phenotype at restrictive temperatures (Oakley and Morris, 1981). The *benA33* mutation alone caused drastic reduction in colony growth at 37°C, and resulted in lethal phe-

notype and prevented colony formation at 42°C (Fig. 1C). The *benA33*; *ebA*Δ double mutant, however, formed a robust colony, although smaller than that formed by the control strain but similar to that of the *ebA*Δ mutant (Fig. 1C). Such a suppression phenomenon was observed at both semi-restrictive and restrictive temperatures of 37°C and 42°C respectively. This result suggested that the MT hyper-stabilization phenotype brought about by the *benA33* mutation was suppressed by the MT destabilization effect caused by the loss of EBA.

Conversely, if EBA's primary function were for stabilizing MTs, the destabilization effect caused by the *ebA*Δ mutation might be compensated by the hyperstabilization effect brought about by the *benA33* mutation. At the permissive temperature of 30°C, the control strain, *benA33* and *ebA*Δ single mutants, as well as the *benA33*; *ebA*Δ double mutant formed colonies in the absence of benomyl (Supplemental Fig. S1). At both permissive and restrictive (42°C) temperatures in the presence of benomyl, the *benA33*; *ebA*Δ double mutant failed to form colonies, demonstrating hypersensitivity to benomyl, as the *ebA*Δ single mutant. In other words, the double mutant did not result any improved growth compared to the *ebA*Δ single mutant. This result indicated that the *benA33* mutation could not suppress the hypersensitivity to benomyl caused by the *ebA*Δ null mutation. Thus, the EBA protein functions not only in MT stabilization, but also in other aspects associated with cytoplasmic MTs.

Plus end-tracking activity of EBA and CLIPA

When the only EBA protein was expressed in fusion with the GFP under the control of its native promoter, EBA–GFP exhibited a typical +TIP localization pattern (Supplemental Fig. S2A). Although the comet-like signals at MT plus ends distributed along the apical cell, they all showed robust motility towards the hyphal apex in the apical cell (Supplemental Movie S1). This result indicated that in *A. nidulans* MT polymerization took place from posterior locations and the hyphal apex did not possess the MTOC activity. The pattern was very similar to that exhibited by a CLIPA fusion with the fluorescent protein mCherry which was the only CLIPA expressed in the strain (Supplemental Fig. S2B, Supplemental Movie S2), similarly to what was reported by the GFP–CLIPA fusion published before (Efimov *et al.*, 2006). Both the EBA–GFP and CLIPA–mCherry signals disappeared rapidly as soon as they made contacts with the hyphal apex, presumably they fell off the MT plus ends when the polymerizing plus ends encountered the plasma membrane or other obstacles. The EBA signal decorated the polymerizing plus ends of cytoplasmic MTs reported by a CFP–tubulin fusion protein (Supplemental Fig. S3).

Because the EB1 family proteins possess the C-terminal EEY/F motif that mediates the interaction with the

N-terminal CAP-Gly motif of the CLIP170 family proteins (Akhmanova and Steinmetz, 2010), we tested whether the positions of the fluorescent protein tags in EBA would affect the MT plus end localization of CLIPA. Indeed, it has been shown that the GFP tag could affect the function of EB1 when it was placed at either N- or C-terminus (Skube *et al.*, 2010). At first, we generated a strain in which EBA–GFP and CLIPA–mCherry were expressed under their native promoters. In its apical cells, however, only EBA–GFP but not CLIPA–mCherry signals were observed at MT plus ends (Fig. 2A). Conversely, GFP was fused to the N-terminus of EBA and the GFP–EBA fusion was expressed under the control of the *alcA* promoter. The plus end-tracking activity was retained by GFP–EBA (Fig. 2B). A published report showed the disappearance of CLIP170 localization at MT plus ends when EB1 was tagged with GFP at either end in cultured animal cells (Skube *et al.*, 2010). We assumed that the mCherry tag would not affect CLIPA's binding to EBA because the CAP-Gly motif is located at the N-terminus of CLIPA (Efimov *et al.*, 2006). So when EBA was expressed with the GFP tag at the C-terminus, the cause of lacking the CLIPA–mCherry signal might be due to the GFP tag that blocked the interaction between EBA's EEY/F motif and CLIPA's CAP-Gly motif. We wanted to test whether the GFP–EBA fusion would affect the localization of CLIPA by generating a strain expressing GFP–EBA and CLIPA–mCherry simultaneously. Both signals appeared at the polymerizing MT plus ends and overlapped completely with each other (Fig. 2B). This result suggests that the exposed C-terminus of EBA is critical for the +TIP activity of CLIPA.

The different impacts of N- and C-terminal GFP fusion of EBA on CLIPA localization prompted us to test whether the fusion proteins were functional. We compared colony growth of strains expressing either GFP–EBA or EBA–GFP by using the wild-type EBA and *ebA*Δ mutant as references. Clear difference was observed when benomyl was supplied at 0.2 μg ml⁻¹ as the colony growth of the *ebA*Δ strain was seriously inhibited (Fig. 2C). At this concentration, strains expressing either GFP–EBA or EBA–GFP formed large conidiating colonies that were relatively smaller than that of the wild-type EBA control (Fig. 2C). Because both GFP–EBA and EBA–GFP were the only full-length EBA proteins expressed in the corresponding strains, this result suggested that both GFP fusion proteins of EBA were partially functional.

We further tested whether the fluorescent protein tags at N- or C-terminal end of EBA and CLIPA would affect the polymerization behaviour of cytoplasmic MTs in apical cells. The Kymograph tool was applied to analyse the motility of MT plus ends (Fig. 3). Because the GFP–EBA fusion did not alter the localization of CLIPA–mCherry, we first measured the polymerization rates based on these two fusions. The comets of GFP–EBA and CLIPA–

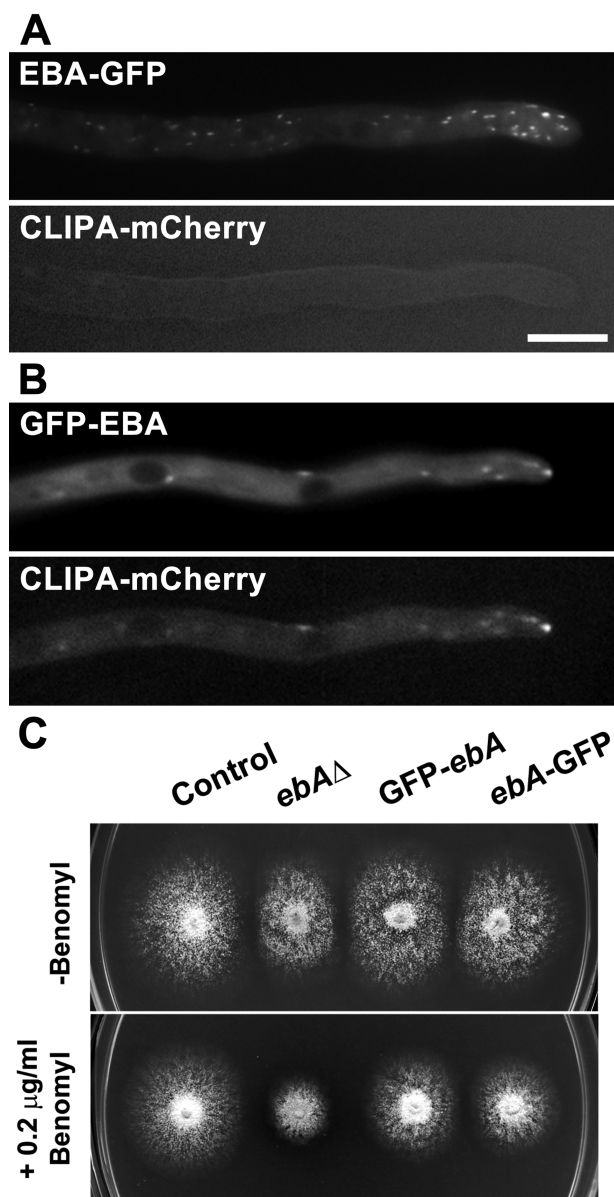


Fig. 2. GFP tagging at the C-terminus of EBA abolishes CLIPA localization. A. CLIPA-mCherry fails to decorate MT plus ends while EBA-GFP prominently appears in comet-like signals. B. GFP-EBA and CLIPA-mCherry colocalize at polymerizing MT plus ends. C. Both GFP-EBA and EBA-GFP are partially functional as the GFP-*ebA* (LBA65) and *ebA*-GFP (RSA318) colonies are significantly larger than the *ebA*Δ mutant (LBA66) but smaller than the control (R153). Scale bar, 5 μm.

mCherry migrated towards hyphal apex at 9.74 ± 2.12 and $10.90 \pm 5.02 \mu\text{m min}^{-1}$ respectively (Fig. 3). We compared these rates to that of MT polymerization in the presence of the native EBA under our experimental condition. We determined that cytoplasmic MTs polymerized at an average rate of $13.11 \mu\text{m min}^{-1}$ when a GFP-TUBA

was used as a marker. This is comparable to a measured rate of $13.73 \mu\text{m min}^{-1}$ in a report when an identical fusion was used (Han *et al.*, 2001). The MT polymerization rate, marked by GFP-EBA, dropped to $5.49 \pm 2.30 \mu\text{m min}^{-1}$ in the *clipA*Δ mutation background (Fig. 3). The drastic difference of MT polymerization rates in the CLIPA-mCherry strain and *clipA*Δ mutant further indicated that the CLIPA-mCherry fusion protein was functional. Because the C-terminal EBA-GFP fusion abolished CLIPA localization at MT plus ends, we measured the migration rate of EBA-GFP in the presence of CLIPA and found it dropped to $6.23 \pm 1.72 \mu\text{m min}^{-1}$, markedly slower than that of the GFP-EBA fusion. This result suggested that the reduced MT polymerization rate in strains expressing EBA-GFP could be caused by the absence of CLIPA at MT plus ends. In contrast, the N-terminal GFP fusion of CLIPA did not alter the polymerization rate significantly, exhibited a rate of $9.56 \pm 1.64 \mu\text{m min}^{-1}$. We then examined MT polymerization rate in the *ebA*Δ mutant and found that the rates dropped to $6.11 \pm 3.66 \mu\text{m min}^{-1}$, indicating significant function of EBA in promoting MT polymerization.

EBA is required for MT plus end-tracking of CLIPA, KipA, and AlpA

We further tested whether EBA and CLIPA depended on each other for their localization at the polymerizing MT

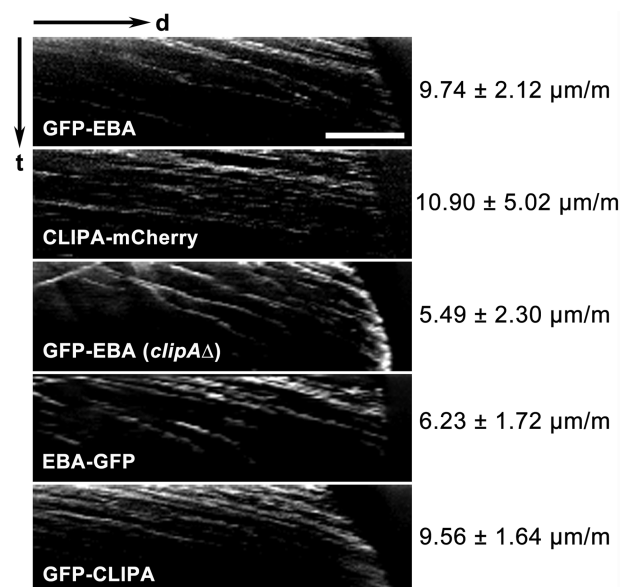
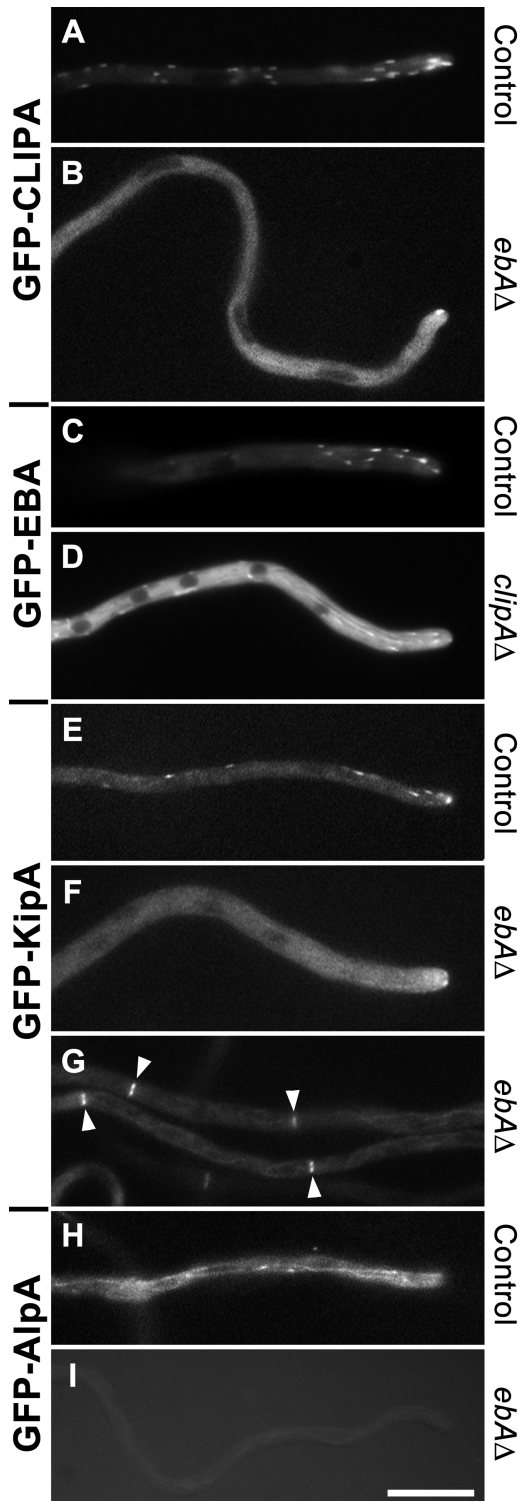


Fig. 3. MT polymerization towards hyphal apices as marked by EBA or CLIPA. Kymograph images demonstrate histories of MT polymerization with the x-axis reflecting the distance and y-axis for time (total 165 s). GFP-EBA, CLIPA-mCherry, and GFP-CLIPA render polymerization rates of $\sim 10 \mu\text{m m}^{-1}$. The polymerization rate marked by GFP-EBA was significantly reduced in the absence of CLIPA. EBA-GFP fusion results in a serious reduction of polymerization rate as well. Scale bar, 10 μm.



plus ends. In strains carrying the *ebAΔ* mutation, the GFP–CLIPA signal became largely diffuse across the cytoplasm in contrast to the rich MT plus end-decorating localization in control cells (Fig. 4A and B). In the *ebAΔ* mutant, the GFP–CLIPA signal sometimes accumulated

Fig. 4. EBA-dependent localization of +TIPs.

A and B. Prominent GFP–CLIPA localization at polymerizing MT plus ends in control cells is replaced by diffuse signals in the cytoplasm in *ebAΔ* mutation background.

C and D. GFP–EBA signals at MT plus ends seen in the control cell are reduced in the cell bearing the *clipAΔ* mutation. Increased diffuse signals also are seen in the cytosol.

E–G. GFP–KipA behaves as a +TIP in the control cell. It appears evenly in the cytoplasm in the *ebAΔ* mutation background.

However, GFP–KipA localization at the septation sites (arrowheads) is independent to EBA.

H and I. GFP–AlpA localization at MT plus ends and along MTs, seen in the control cell, is completely abolished by the *ebAΔ* mutation. Scale bar, 10 μ m.

near the hyphal apex (Fig. 5B), but never appeared in comet-like patterns. Thus, it suggests that the normal MT plus end-tracking activity of CLIPA is dependent on EBA. We also examined whether CLIPA played a role in regulating the dynamics of EBA. In the absence of CLIPA, the GFP–EBA signal still appeared at MT plus ends, concomitant with increased diffuse signals in the cytoplasm (Fig. 4C and D). To quantify these different distribution patterns of GFP–EBA, we measured the ratio of fluorescent intensities of the comet-localized and the cytoplasmic diffuse signals. The ratio was 1.85 in the control cells and dropped to 1.34 in *clipAΔ* cells. This result suggested that CLIPA might play a role in facilitating EBA's MT plus end-tracking activity, which could be linked to its function in promoting MT plus end polymerization rate.

The kinesins reported as +TIPs typically possess the SxI/LP motif in a basic domain rich in serines (Gouveia

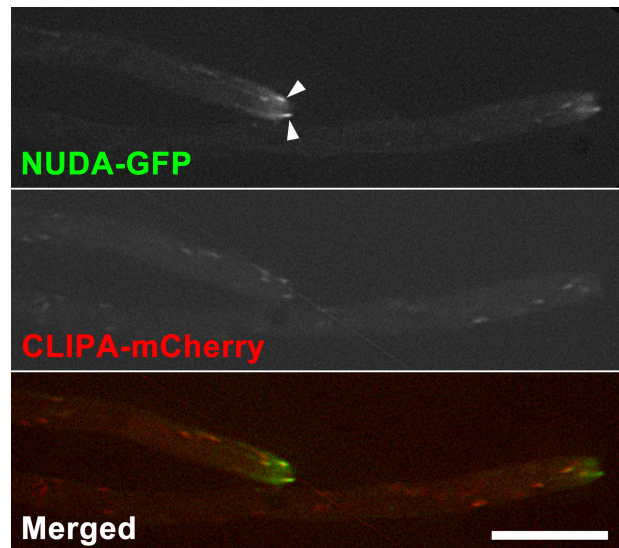


Fig. 5. Differential localization patterns of the dynein NUDA and CLIPA. While CLIPA–mCherry appears evenly at the plus ends of all polymerizing MTs, NUDA–GFP appears prominently at MT plus ends near the hyphal apices. In the merged image, NUDA–GFP appears in green and CLIPA–mCherry in red. Scale bar, 10 μ m.

and Akhmanova, 2010). Similarly, the reported +TIP-behaving kinesin KipA harbours an 'STLP' motif right after the starting methionine. We tested whether the KipA's plus end-tracking activity was dependent on EBA. Compared to its MT plus end-tracking signal, in the *ebaΔ* mutation background, GFP–KipA signal completely disappeared from polymerizing MT plus ends (Fig. 4E and F). Previously, it was reported that KipA decorated the septation site in addition to MT plus ends (Konzack *et al.*, 2005). This localization was preserved when *eba* was knocked out (arrowheads, Fig. 4G). Thus, the septation site localization of KipA is independent of KipA's MT plus end-tracking activity.

We have also tested whether the MT plus end-tracking activity of the AlpA protein, a member of the MT-associated protein XMAP215 family and bearing an 'SSLP' motif towards its N-terminus, was dependent on EBA. Unlike other typical +TIPs, AlpA decorated cytoplasmic MTs instead of being exclusively at the plus end like typical +TIPs (Enke *et al.*, 2007). As reported, the GFP–AlpA signal often covered the MTs completely while being more prominent at MT ends (Fig. 4H). Such a localization pattern was completely abolished in strains carrying *ebaΔ*, and GFP–AlpA became diffused in the cytosol (Fig. 5I). Thus, we concluded that both AlpA and KipA associated with MT plus ends by hitchhiking on EBA.

EBA-dependent and independent localization of cytoplasmic dynein

The cytoplasmic dynein and the associated dynactin complexes exhibit rapid plus end-tracking activity in hyphal tip cells (Han *et al.*, 2001; Zhang *et al.*, 2003). However, the dynein and dynactin signals are typically much more pronounced towards the hyphal apex. This is different from that of EBA or CLIPA which more or less shows consistent localization pattern at all polymerizing plus ends of cytoplasmic MTs. At first, we examined the localization of the dynein heavy chain NUDA and CLIPA in the same cells. Again, the CLIPA–mCherry signal decorated MT plus ends evenly along the apical cell while NUDA–GFP appeared more conspicuously near the apex (arrowheads, Fig. 5). In CLIPA-decorated comets towards posterior parts of the apical cells, there were very weak NUDA signals.

Such differential localization patterns in actively growing hyphal tip cells prompted us to examine whether dynein localization depended on EBA. In published studies in animal cells, it is often stated that dynein localization at MT plus ends is also dependent on EB1 (Akhmanova and Steinmetz, 2008). Again, NUDA–GFP appeared conspicuously as bright comets near the hyphal apex in the control cells (Fig. 6A). Less bright comets were found in posterior regions. These comets continuously migrated towards the

hyphal apex as revealed by Kymograph (kymo, Fig. 6A; Supplemental Movie S3). The tracks were nearly perfectly parallel to each other, reflecting uniform MT polymerization rates in the hyphal apical cells. Noticeably, the comets quickly gained enhanced intensities when they reached close to the hyphal apex (Fig. 6A). When NUDA–GFP was examined in the *ebaΔ* mutation background, it remained to be near the hyphal apex as bright comets with long trailing tails (arrows, Fig. 6B). However, its localization in the posterior regions became diminished so that no obvious tracking trails were visible by kymograph (kymo, Fig. 6B; Supplemental Movie S4). Instead, the NUDA–GFP fluorescent signal was observed in streams towards the hyphal apex (Supplemental Movie S4). This result suggested that NUDA's appearance towards polymerizing MT plus ends near the hyphal apex was independent of its EBA-dependent MT plus end-tracking. Other forces might be responsible for the delivery of cytoplasmic dynein towards the apices.

Because NUDA association with MT plus ends towards the hyphal apex did not require EBA, we asked whether such localization was assisted by CLIPA. GFP–NUDA was examined in the *ebaΔ*; *clipAΔ* double mutation background. Compared to the typical MT plus end-tracking behaviour in the control cells and cells carrying the *ebaΔ* single mutation, GFP–NUDA decorated long segments of cytoplasmic MTs towards the anterior part of the apical cells (Fig. 6C). The signal was more or less evenly distributed along those MTs and did not exhibit any obvious plus end-tracking phenomenon although showed back and forth oscillations (Supplemental Movie S5). No distinct GFP signal was detected after this anterior segment in the apical cell (Fig. 6C). This result further suggests that there was an EBA/CLIPA-independent interaction between dynein and MTs in actively growing hyphal tip cells.

Absence of cytoplasmic dynein, EBA, and CLIPA together does not abolish colony growth

Unlike what has been described in yeast, the *ebaΔ*; *clipAΔ* double mutant was viable and produced robust colonies as described above. In yeast, it was also found that the *eb1* homologue *bim1* had a synthetic lethal interaction with the *dyn1* gene encoding the cytoplasmic dynein heavy chain (Muhua *et al.*, 1998). We further tested how the fungus would respond to the loss of all three important +TIPs. We used the *alcA(p)::GFP–nudA* allele which allows the formation of conidiating colonies upon expression and resembles the *nudAΔ* phenotype when its expression is repressed by including glucose as the carbon source (Xiang *et al.*, 1995). Surprisingly, the *ebaΔ* and *clipAΔ* mutations did not add more severity to the *nudA* single mutant (Fig. 7). In other words, the

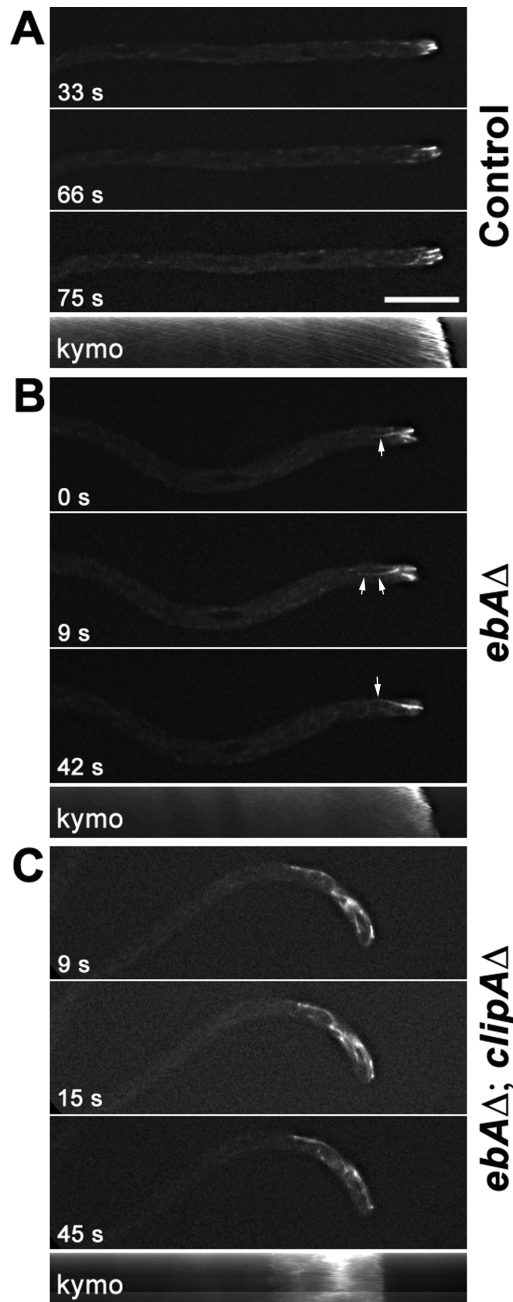


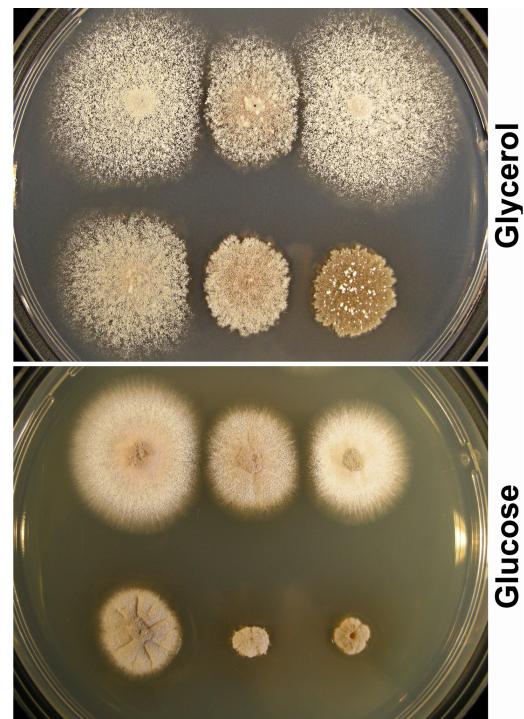
Fig. 6. The MT plus end-tracking activity of NUDA depends on EBA. Time in s is shown on the bottom left.

A. In the control cell, NUDA-GFP appears most conspicuously near the hyphal apex while weaker comet-like signals can be detected elsewhere. The Kymograph (kymo) summarizes the history of the NUDA dynamics with the x-axis represents the distance and y-axis for time (total of 165 s).

B. In the *ebA*Δ mutation background, NUDA continues to appear at MT segments near the hyphal apex. Note that longer segments of MTs are decorated than in the control cell. The plus end-tracking activity is largely abolished as no tracks can be distinguished. Instead, the GFP signal often trails along MTs (arrows). No obvious patterns were detected in the Kymograph image over 165 s.

C. In the *ebA*Δ; *clipA*Δ double mutation background, long segments of disorganized MTs are decorated by NUDA towards the hyphal apex. Linear NUDA-GFP fluorescent signals exhibit oscillatory activities along MTs near the hyphal apex.

Scale bar, 10 μm.



Control	<i>ebA</i>Δ	<i>clipA</i>Δ
<i>ebA</i>Δ; <i>clipA</i>Δ	<i>alcA</i>(p):: <i>nuda</i>	<i>ebA</i>Δ; <i>clipA</i>Δ; <i>alcA</i>(p):: <i>nuda</i>

Fig. 7. The *ebA*, *clipA*, and *nuda* triple mutant is viable. Colonies of the control (R153), *ebA*Δ (LBA66), *clipA*Δ, *ebA*Δ; *clipA*Δ double mutant (RSA13), *alcA*(p)::*nuda* (GFP-dynein), and *ebA*Δ; *clipA*Δ; *alcA*(p)::*nuda* triple mutant are shown on duplicate glycerol (*alcA*(p) inducing) and glucose (*alcA*(p) repressing) plates. The *nuda* mutant has the only *nuda* gene under the control of the *alcA* promoter. *nuda* is expressed on the glycerol medium and repressed on the glucose medium. The *ebA*Δ; *clipA*Δ; *alcA*(p)::*nuda* triple mutant grows similarly as the *alcA*(p)::*nuda* mutant on the glucose medium, forming small 'nud' colonies.

defects caused by the loss of cytoplasmic dynein were much more severe than that caused by the loss of either or both of *ebA* and *clipA*. There were no strong genetic interactions among these three mutations.

Reduced dynamics of cytoplasmic MTs upon the loss of EBA and CLIPA

The synthetic lethality of the null mutations in the yeast *ebA* and *clipA* homologues has prevented the studies of MT dynamics when both +TIPs are absent. Cytoplasmic MTs

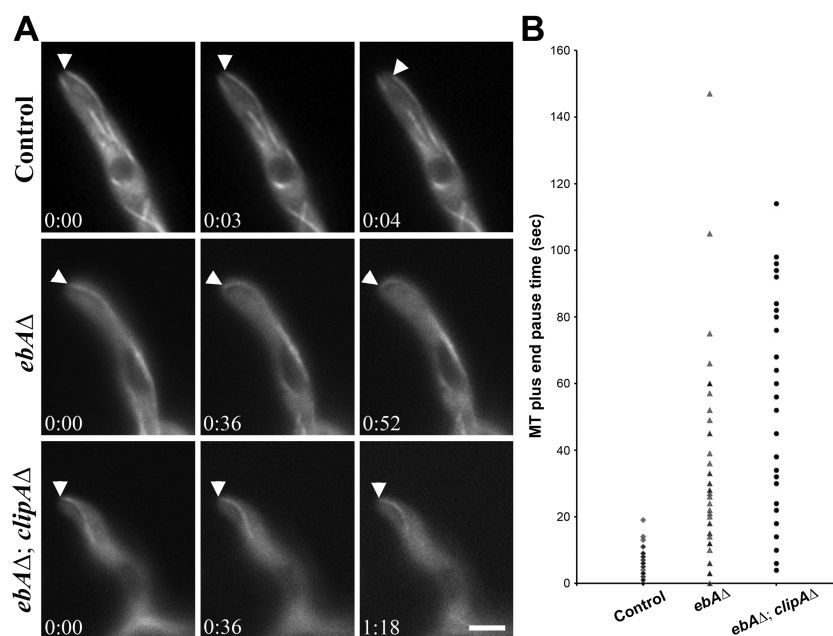


Fig. 8. Prolonged MTs dwelling at hyphal apex upon the loss of +TIPs.

A. Cytoplasmic MTs highlighted by GFP-TUBA are shown in the apical cells of the control (GFP-tubulin), *ebAΔ* single mutant (RSA29), and *ebAΔ; clipAΔ* double mutant (RSA323) cells. Time in 'min:s' is shown on the bottom left. Scale bar, 2 μ m.

B. Distribution of the pause times exhibited by MT plus ends in the apical cells of the control, *ebAΔ* single mutant, and *ebAΔ; clipAΔ* double mutant.

polymerize robustly towards the hyphal apex and shrink rapidly upon encountering the plasma membrane vicinities in the apical cells (Han *et al.*, 2001; Horio and Oakley, 2005). We tested whether the absence of these +TIPs would affect such behaviours. In control cells, again, multiple cytoplasmic MTs rapidly shortened upon reaching the apex, usually within a few seconds (control, Fig. 8A; Supplemental Movie S6). In the *ebAΔ* background, however, one or two MTs reached to the apex but remained to be associated with the apex (pause) for as long as a minute or more (Fig. 8A; Supplemental Movie S7). In the *ebAΔ; clipAΔ* double mutation background, again, cytoplasmic MTs often paused for a minute or longer at the hyphal apex (Fig. 8A; Supplemental Movie S8). Such a long duration of MT attachment to the apex was often concomitant with the bending the apical cell. Collectively, in the control apical cells, cytoplasmic MTs in all examined cells shrunk rapidly with pause times within 20 s that were averaged at 6.13 s ($n = 30$) (Fig. 8B). In either the *ebAΔ* single or the *ebAΔ; clipAΔ* double mutation background, cytoplasmic MTs exhibited pause times in wide ranges. In *ebAΔ*, they have an average pause time of 33.93 s ($n = 42$); and in the *ebAΔ; clipAΔ* double mutant, the pause times were averaged at 55.97 s ($n = 36$). Thus, in addition to missing EBA, the absence of CLIPA resulted in even longer pause time for cytoplasmic MTs.

Discussion

Our results showed that in hyphal tip cells EBA acted as a key mediator for the dynamic interaction between other +TIPs and the plus ends of cytoplasmic MTs that robustly

polymerized towards the apex in *A. nidulans*. The EBA-mediated interaction between +TIPs and polymerizing MT plus ends was critical for sustained directional tip expansion during rapid growth of hyphal apical cells. However, the MT plus end-tracking activity was not required for the function of cytoplasmic dynein in driving nuclear migration and in colony growth as well as conidiation. Furthermore, in the absence of three prominent +TIPs, EBA, CLIPA, and NUDA, hyphal cells continued to grow and divide to form colonies although at much reduced rates. EBA and CLIPA are critical factors that regulate robust dynamics of cytoplasmic MTs in actively growth tip cells. But intrinsic activities of MTs and contributions of MAPs acting at sites other than the plus end are sufficient to support growth at limited scales in filamentous fungi like *A. nidulans*.

+TIPs and sustained unidirectional expansion of hyphal apical cells

In actively growing hyphal apical cells, MTs are essential for rapid and steady tip growth as demonstrated earlier (Riquelme *et al.*, 2003; Horio and Oakley, 2005; Horio, 2007). Here we showed that EBA regulated the behaviour of polymerizing MT plus ends that influenced directional expansion of hyphal tips. EBA not only acted as an MT-stabilizing factor as its loss led to hypersensitivities to the MT-depolymerizing agent benomyl, it also played a critical role in endorsing the rapid shrinkage of MT plus ends once cytoplasmic MTs reach the apex of the apical cell. A similar phenomenon was observed in budding yeast cells lacking the EBA orthologue Bim1p in which MTs depolymerized slower and took longer pauses when com-

pared to wild-type cells (Tirnauer *et al.*, 1999). In the *ebaΔ* mutant cells, cytoplasmic MTs frequently exhibited significant longer pause times, often 10 times longer than that in control cells. In addition, we also observed that these cells produced few cytoplasmic MTs in the apical cell. We propose that rapid turnovers of cytoplasmic MTs are critical for generating new MTs. Continuous polymerization of cytoplasmic MTs towards the hyphal apex is required for the tip cell to undergo sustained unidirectional growth.

In addition to EBA, a number of other +TIPs as well as the cell end marker Tea proteins also are required for sustained unidirectional expansion of the hyphal tip cell (Konzack *et al.*, 2005; Efimov *et al.*, 2006; Enke *et al.*, 2007; Higashitsuji *et al.*, 2009; Takeshita and Fischer, 2011). Their mutants form wavy hyphae with regular undulating patterns, although at different degrees. Here we found that EBA was required for the plus end localization of the MT polymerase AlpA. AlpA interacts directly with the cell end marker TeaA and the interaction allows the convergence of cytoplasmic MTs upon reaching the apex (Takeshita *et al.*, 2013). When AlpA was no longer localized to MT plus end, therefore, we expected that MTs were not converged effectively to support unidirectional growth in hyphal apical cells. Because the loss of proteins like CLIPA does not abolish the MT plus end tracking activity of EBA, their functions in regulating directional growth are likely independent of EBA. In other words, different defects in MT dynamics could contribute to altering directional growth at the hyphal apex. Such a defect is likely different from that caused by the loss of the motor Myosin V that does not lead to forming hyphae with regular wavy appearance but to significant loss of growth robustness (Zhang *et al.*, 2011; Taheri-Taleh *et al.*, 2012). Again, together with these findings our data further support the notion that cytoplasmic MTs play critical roles in supporting unidirectional growth of hyphal apical cells, likely with the assistance of proteins specifically acting at polymerizing MT plus ends.

Synergetic functions of +TIPs for MT dynamics

The EB1 proteins generally are considered to form the core of +TIPs and are essential for others to interact with MT plus ends (Jiang and Akhmanova, 2011; Mimori-Kiyosue, 2011). Indeed, the MT plus end localization of most +TIPs is dependent on EB1 either through the interaction with the C-terminal EEY/F motif via the CAP-Gly domain or with the EB1 homology (EBH) domain via the SxIP motif (Akhmanova and Steinmetz, 2010). For example, the animal CLIP170 requires EB1 for its MT plus end-tracking activity (Bieling *et al.*, 2008; Dixit *et al.*, 2009). These principles are applicable in *A. nidulans* as the MT plus end localization of the CAP-Gly protein CLIPA as well as those of Sxl/LP motif proteins KipA and AlpA

were dependent on EBA. However, it remains to be tested experimentally whether KipA and AlpA directly interact with EBA to warrant a hitchhiking association with MT plus ends. We found that the addition of a GFP tag at the C-terminus of EBA would abolish the localization of CLIPA. Similar findings were reported for their human counterparts (Skube *et al.*, 2010). Such an EB1-dependent localization phenomenon often leaves the impression that functions of these +TIPs are completely dependent on their interaction with EB1. Here we showed that the CLIP170 homologue CLIPA, although not required for EBA's MT plus end-tracking activity, plays a significant role to promote MT plus end polymerization and likely enhances EBA's interaction with MT plus ends. Such a function is critical for hyphal apex to sustain the momentum of directional expansion (Efimov *et al.*, 2006). Moreover, the *ebaΔ*; *clipAΔ* double mutant exhibited more severe phenotypes in hyphal and colony growth than the *ebaΔ* single mutant even though CLIPA no longer localized to the MT plus ends in the absence of EBA. This result further suggests that CLIPA functions beyond the MT plus end and such a function is critical for hyphal growth.

Bearing intrinsic MT association activities, factors like CLIPA and KipA would be able to interact with cytoplasmic MTs themselves. Although their functions in regulating the behaviour of cytoplasmic MTs may be primarily dependent on their MT plus ends tracking activity which is dependent on EBA, they may interact with MTs in the absence of EBA and exert a regulatory role. Their functions may be cooperative with that of EBA. This is consistent with the finding that the *clipA* null mutant showed few MTs that reached to hyphal apex through polymerization and were less likely to undergo catastrophe compared to those in wild-type cells (Efimov *et al.*, 2006). A similar conclusion was drawn for its homologue Bik1 in budding yeast (Blake-Hodek *et al.*, 2010). Our results further strengthen the notion that EBA and CLIPA play synergistic roles in promoting MT dynamics. Such a synergistic role goes beyond EB1 and CLIP170 as other +TIPs like XMAP215 and Sentin also play cooperative roles in promoting MT dynamics in animal cells (Li *et al.*, 2012). Interestingly, only *ebaΔ* but not *clipAΔ* exhibited the phenotype of benomyl hypersensitivity, suggesting that EBA likely plays a more significant role in stabilizing MTs than CLIPA. Such a stabilizing function goes beyond simply preventing an MT from depolymerization. For example, it is known that the EB1 proteins can stimulate MT nucleation and promote both rescue and catastrophe events *in vitro* (Vitre *et al.*, 2008). Our *in vivo* results agree with this *in vitro* finding. In the absence of EBA, we found that there were fewer cytoplasmic MTs, similar to what has been reported in another ascomycete *Neurospora crassa* (Mourino-Perez *et al.*, 2013). Such a phenotype could be caused by reduced MT nucleation events. Furthermore, as suggested by the *in vitro* data, long pauses of a few

cytoplasmic MTs in the *ebAΔ* hyphae could be resulted from reduced MT turnover rates. Rapid turnovers regulated by both EBA and CLIPA are critical for the remodelling of cytoplasmic MTs. Without sufficient number of new MTs generated, the MT cytoskeleton would become more vulnerable to depolymerizing challenges like benomyl treatment.

The synergistic functions of homologues of EB1 and CLIP170 also are evidenced by the results that in budding yeast mutations in the two corresponding genes cause synthetic lethality (Schwartz *et al.*, 1997). In *A. nidulans*, the *clipAΔ* mutation enhanced hyphal growth defects caused by the *ebAΔ* mutation, but the double mutant still produced conidiating colonies. This suggests that additional factors play redundant roles as these two dominant +TIPs in this filamentous fungus. One of such factors could be cytoplasmic dynein. In budding yeast, the dynein *dhc1* mutation shows a synthetic lethality interaction with the *bim1/yeb1* mutation (Muhua *et al.*, 1998). In *A. nidulans*, the loss of NUDA leads to a drop of MT catastrophe rate (Han *et al.*, 2001), similar to what has been observed in the *clipA* mutant cells. The phenotype of the triple mutant did not allow us to further pursue such redundant roles because the mutant formed colonies similar to those of *nudA* single mutant, which are extremely small in size and failed to conidiate (Xiang *et al.*, 1994). It is intriguing that despite the importance of the +TIPs of EBA, CLIPA, and cytoplasmic dynein, hyphae continued to grow and colonies were formed in the absence of all three factors. Thus, either intrinsic properties of MTs or functions of other MT regulatory factors would allow the fungus to grow under such a circumstance.

Discrepancies are found about whether the MT plus end-tracking activity of the XMAP215/TOG proteins requires the EB1 family proteins. For example, in fission yeast the homologous Alp14 protein as a microtubule polymerase tracks at MT plus ends, independently to the EB1 homologue Mal3 (Al-Bassam *et al.*, 2012). However, in *Drosophila* the homologous MSPS protein depends on EB1 for its MT plus end-tracking activity (Currie *et al.*, 2011), which is similar to what we found here. Moreover, in budding yeast the kinesin Kip2 which forms a complex with the CLIP170 homologue Bik1 and tracks MT plus ends (Carvalho *et al.*, 2004). Furthermore, it has been shown that dynein localization to the MT plus end is not dependent on Bim1 in this organism (Carvalho *et al.*, 2004; Markus *et al.*, 2009). Thus, variations are expected in regard to how different +TIPs are engaged in regulating MT plus end dynamics and perform distinct cellular activities in different systems.

As the list of +TIPs grows, especially those associated with EB1 (Yu *et al.*, 2011; Jiang *et al.*, 2012), it is intriguing how the very fine MT plus end can harbour so many proteins and harness their divergent functions to modulate

its dynamics. For example, their functions can be either synergetic (e.g. EB1, XMAP215, and Sentin) or antagonistic (i.e. XMAP215 and the XKCM1 kinesin) (Kinoshita *et al.*, 2001; Li *et al.*, 2012; Zanic *et al.*, 2013). Furthermore, unlike what was described here that colonies were produced by mitosis and hyphal expansion in the absence of EBA, CLIPA, and cytoplasmic dynein all together in *A. nidulans*, knocking down of EB1 alone would already jeopardize cell division and other MT-regulated cell behaviours in *Drosophila* (Rogers *et al.*, 2002). In general, more complex scenarios are expected in multicellular organisms than in unicellular ones. The +TIPs investigated here showed their characteristic localization patterns although all tracked at MT plus ends. Future *in vitro* reconstitution experiments would be informative for us to understand how these factors are engaged together at MT plus ends.

Dynein's function in nuclear migration is independent of MT plus end-tracking

In filamentous fungi, cytoplasmic dynein is the primary motor for nuclear migration in growing hyphae (Plamann *et al.*, 1994; Xiang *et al.*, 1994). Proteins of the dynein complex as well as its regulators like dynactin and NUDF/LIS1 all exhibit prominent localization at polymerizing MT plus ends, especially towards the hyphal apex (Han *et al.*, 2001; Zhang *et al.*, 2003). Apparently, both the localization pattern and the nuclear migration role are conserved in animal systems (Vaughan *et al.*, 1999; Fridolfsson and Starr, 2010; Tsai *et al.*, 2010). An outstanding question was whether the dynein molecules associated with MT plus ends contribute to nuclear migration. In budding yeast, dynein is targeted to MT plus ends by the +TIP Bik1 and the LIS1 homologue Pac1 to drive the nucleus towards the bud neck after the motor is delivered to the bud cortex (Lee *et al.*, 2003; Sheeman *et al.*, 2003). This suggests that the MT plus end-tracking activity might be important for nuclear migration. In this study, we showed that MT plus end tracking activity was largely lost in the absence of EBA, except near the hyphal apex. However, the *ebAΔ* mutant formed robust and conidiating colonies with no noticeable defects in nuclear distribution (data not shown), similarly to what has been described in the *clipAΔ* mutant (Efimov *et al.*, 2006). Defects in dynein and consequently nuclear distribution typically lead to the formation of small and non-conidiating 'nud' colonies (Xiang *et al.*, 1994). Hence, we concluded that dynein motors that tracked at most MT polymerizing plus ends were not essential for nuclear migration. However, our study did not rule out a possible contribution of the dynein motors at the MT plus ends near the hyphal apex in nuclear migration.

Our study also left a question regarding how dynein still appeared conspicuously at the plus end of the cytoplasmic MTs that reached close to the apical dome of the

Table 1. *A. nidulans* strains used in this study.

Strain	Genotype	Source
AHA2	<i>alcA(p)::GFP-EBA::pyrG; pabaA1 yA2; pyrG89</i>	This study
CZA20	<i>ebA-GFP::AfpYrG; pyrG89; pyroA4; nkuA::argB; riboB2</i>	This study
CZA37	<i>nudA-GFP; clipA-mCherry::AfpYrA; pyroA4</i>	This study
CZA60	<i>clipA-mCherry::AfpYrA; pyrG89; pyroA4; nkuA::argB</i>	This study
ΔclipA	<i>pyrG89; pyroA4; wA2; clipAΔ::pyroA</i>	Efimov <i>et al.</i> (2006)
GFP-clipA	<i>alcA(p)::GFP-clipA::pyr4; pyrG89; pyroA4; wA2</i>	Efimov <i>et al.</i> (2006)
GFP-dynein	<i>alcA(p)::GFP-nudA::pyr4; pyrG89; pyroA4; wA2</i>	Xiang <i>et al.</i> (2000)
GFP-tubulin	<i>alcA(p)::GFP-tubA::pyr4; pyrG89; pyroA4; wA2</i>	Han <i>et al.</i> (2001)
GR5	<i>pyrG89; pyroA4; wA2</i>	FGSC
LBA62	<i>alcA(p)::GFP-nudA::pyr4; ebAΔ::pyrG; wA2</i>	This study
LBA65	<i>alcA(p)::GFP-ebA::pyrG; pyrG89; pyroA4; wA2</i>	This study
LBA66	<i>ebAΔ::pyrG; pyroA4; pyrG89; wA2</i>	This study
LBA74	<i>alcA(p)::CFP-tubA::pyr4; alcA(p)::GFP-EB1::pyrG; pyrG89; wA2</i>	This study
R153	<i>pyroA4; wA2</i>	FGSC
RSA13	<i>ebAΔ::pyrG; wA2; pyrG89; pyroA4; clipAΔ::pyroA</i>	This study
RSA29	<i>alcA(p)::GFP-tubA::pyr4; ebAΔ::pyrG; pyrG89</i>	This study
RSA71	<i>ebAΔ::pyrG; alcA(p)::GFP-clipA; wA2; pyroA4</i>	This study
RSA73	<i>clipAΔ::pyroA; alcA(p)::GFP-ebA::pyrG; pyroA4; pyrG89</i>	This study
RSA75	<i>ebAΔ::pyrG; benA33; wA2</i>	This study
RSA77	<i>ebAΔ::pyrG; alcA(p)::GFP-kipA::pyr4; wA2</i>	This study
RSA103	<i>alcA(p)::GFP-<i>alpA</i>::pyr4; pyrG89; pabaA1 yA2</i>	This study
RSA107	<i>alcA(p)::GFP-<i>alpA</i>::pyr4; ebAΔ::pyrG</i>	This study
RSA197	<i>benA33; pyrG89; pabaA1 yA2</i>	This study
RSA233	<i>alcA(p)::GFP-nudA::pyr4; clipAΔ::pyroA; ebAΔ::pyrG; pyroA4; pyrG89</i>	This study
RSA255	<i>GFP-nudA; clipAΔ::pyroA; ebAΔ::pyrG; pyroA4; pyrG89</i>	This study
RSA318	<i>ebA-GFP::AfpYrG; clipA-mCherry::AfpYrA; pyrG89; pyroA4; wA2</i>	This study
RSA323	<i>clipAΔ::pyroA; ebAΔ::pyrG; alcA(p)::GFP-tubA::pyr4; pyroA4; pyrG89; wA2</i>	This study
RSA343	<i>clipA::mCherry::AfpYrA; alcA(p)::GFP-ebA::pyrG; pyrG89; pyroA4; nkuA::argB</i>	This study
SSK92	GR5 transformed with pSK82 [GFP-KipA]	Konzack <i>et al.</i> (2005)
TN02A7	<i>pyrG89; pyroA4; nkuA::argB; riboB2</i>	Nayak <i>et al.</i> (2006)

FGSC, Fungal Genetics Stock Center.

hyphal cells in the *ebAΔ* mutant. Apparently, the motor did not arrive there through hitchhiking MT plus end. Instead, it is likely delivered by the kinesin motor KinA as demonstrated previously (Zhang *et al.*, 2003). Long segments of MTs towards the apex were highlighted by dynein when both EBA and CLIPA were absent. This was likely caused by the prolonged dwelling time of MT plus ends when they reached the apex. Dynein there has been shown to play critical roles in transporting endosomes in the retrograde manner (Zhang *et al.*, 2010). Therefore, the cytoplasmic dynein motor is engaged in distinct mechanisms to power fundamental motile events from endosome trafficking to nuclear migration in fungal hyphae as well as animal cells.

Experimental procedures

A. nidulans strains and growth conditions

Aspergillus nidulans strains used in this study are listed in Table 1. The strains were inoculated on rich and minimal media according to published protocols (Kafer, 1977; Liu and Morris, 2000). Strains bearing *alcA(p)*-fused genes were inoculated on minimal media with glycerol as the sole carbon source for inducing their expression at modest levels, and on minimal or rich media with glucose in order to turn off the expression of genes of interest. Standard crosses were

carried out to generate mutants with desired genotypes. All strains were streaked to single colonies for three times before being used for further analysis. Transformation experiments were carried out as described in a published work (Osmani *et al.*, 1987).

In the test of sensitivities to MT depolymerization, benomyl (Sigma) was added to growth media at designated concentrations prior to inoculation of conidial spores.

Recombinant DNA techniques employed in this study

Fragments of targeted genes were amplified from genomic DNA by polymerase chain reaction (PCR) using the Accuprime Pfx DNA polymerase (Invitrogen) and gel-purified using QIAquick gel extraction kit (Qiagen). Primers used in this study are listed in Supplemental Table S1. The plasmid for standard cloning was pBluescript KS+ (Stratagene) and host bacterial strain was DH5α unless mentioned otherwise.

Cassettes used for targeted gene deletion and tagging were made according to published protocols of fusion PCR (Nayak *et al.*, 2006; Szewczyk *et al.*, 2006). The *Aspergillus fumigatus* *pyrG*, *pyroA*, and *riboB* genes (Nayak *et al.*, 2006) were used as the markers for autotrophic selection during transformations. The FNO3 plasmid containing the green fluorescent protein (GFP)-coding sequence and *AfpYrG* gene was used for GFP tagging to the C-terminus of a targeted protein (Szewczyk *et al.*, 2006). In order to tag proteins with the mCherry fluorescent protein at the C-terminus, we con-

structed the pLB14 plasmid. Briefly, the mCherry-coding sequence was amplified by PCR using the primers of cherry5B and cherry3RI from the pRSET-B plasmid (Shaner *et al.*, 2004). The PCR product was digested by BamHI and EcoRI and cloned into the *AfpyroA* plasmid at the corresponding sites to give rise to pLB14.

For tagging target genes with GFP or mCherry-coding sequence at the N-terminus and controlling the expression by *alcA(p)*, pLB04 with *A. nidulans pyrG* and pJK13 with *A. fumigatus pyrG* marker genes were used, respectively, as the backbone for cloning the 5' truncated region of the genes of interest (Kim *et al.*, 2006; 2009). We also used pJK16 [*alcA(p)::mCherry::AfpyroA*] and pJK20 [*alcA(p)::GFP::AfpyroA*] which contained the *A. fumigatus pyroA* gene as the selection marker for similar genetic manipulations. To construct pJK16, the pAlc-mCherry plasmid (Kim *et al.*, 2009) was digested with NotI and filled in with nucleotides to become blunt-ended, and digested with SacI. The *A. fumigatus pyroA* fragment was derived from the *AfpyroA* plasmid by digestion with HindIII and then being blunt-ended, followed by digestion with SacI. The resulting *AfpyroA* fragment was cloned into the digested pAlc-mCherry plasmid by DNA ligation reaction. To construct pJK20, the pLB04 plasmid was digested with BamHI and HindIII to excise the *pyrG* fragment before being used as the cloning backbone. The *AfpyroA* fragment was excised from the *AfpyroA* plasmid by digestion with BamHI and HindIII. Ligation of the two resulting fragments gave rise to pJK20.

Genetic manipulations of the *ebA* and *clipA* genes

In order to generate an *ebA*Δ strain, the 5' and 3' flanking regions of the *ebA*-coding sequence were amplified by primer pairs of DEB155b + DEB153la and DEB135B + DEB133X respectively. The resulting 5' *ebA*-flanking fragment was digested by the restriction enzymes EcoRV + EcoRI, and the 3' fragment by enzymes BamHI + XbaI. These two fragments were subsequently cloned into the pXX1 plasmid (Xiang *et al.*, 1995) containing the *pyrG* gene at the corresponding sites to give rise to the plasmid pXX1-EB153. The deletion cassette DNA was amplified by primers of DEB155b and DEB133X using pXX1-EB153 as the template, and used for transformation into the host GR5.

The *alcA(p)::GFP-ebA* strain was generated by transforming a recombinant plasmid as described below. Briefly, a fragment of the *EBA*-coding region towards the 5' end was amplified using the primers AnEB15X and AnEB13B. The amplified fragment was gel-purified and digested with the restriction enzymes XbaI and BamHI, and cloned into the pLB04B plasmid (Kim *et al.*, 2006) at the corresponding sites to give rise to the pLB04B-EB1 plasmid for transformation into the host GR5.

In order to tag the *EBA* protein with GFP at the C-terminus, a 3' coding region of the *ebA* gene and a flanking region were amplified using primer pairs of 2682B + 2682C and 2682D + 2682E, respectively, and genomic DNA as the template. Note that the stop codon of the *ebA* gene was not included in the primer 2682C so that the amplified 3' fragment would have codons in frame with the GFP-coding sequence after fusion. The tandem GFP plus *AfpyrG* fragment was amplified using the pFNO3 plasmid as the template and primers of FNGFP-Fd and UFG3RV. The fusion cassette was

made by combining these three fragments using primers of 2682A and DEB133X according to a published protocol (Nayak *et al.*, 2006).

A similar strategy was taken to tag the CLIPA protein with mCherry at the C-terminus under the control of the native *clipA* promoter. The primers used were 1475B + 1475C and 1475D + 1475E pairs. The tandem mCherry and *AfpyroA* sequence was amplified from the pLB14 by using primers of cherry5B and *AfpyroA3*. The resulting three fragments were integrated together to form the tagging cassette by fusion PCR using primers of 1475A and 1475F. The TN02A7 strain was used in both C-terminal GFP/mCherry-tagging transformation experiments.

Fluorescence microscopy and imaging

Conidial spores of desired strains were inoculated on solid media for producing germlings containing actively growing tip cells. Agar blocks containing the germlings were excised from Petri dishes and gently laid down on coverslips prior to being transferred to an Axiovert 200 fluorescent microscope (Carl Zeiss). Images were acquired using a Plan Fluor 100× objective. The GFP and mCherry signals were observed using ET GFP (Cat # 49002) and ET Texas Red (Cat # 49008) filter sets (Chroma). A DualView device equipped with corresponding filters (Photometrics) was used to simultaneously observe of both GFP and mCherry signals. Images were acquired using the Metamorph software package (Molecular Devices) and analysed by the Kymograph tool included. Micrographs were assembled in Photoshop (Adobe Systems) for presentation.

Acknowledgements

This report is based on the study supported in part by the National Science Foundation (NSF) under the Grant MCB-0615892, the UC MEXUS-CONACYT Collaborative Grant CN-04-95, and USDA-NIFA under the project CA-D-PLB-6542-H. Any opinions, findings, and conclusions or recommendations expressed in this material are those of the authors and do not necessarily reflect the views of the funding agencies. CJTZ was a trainee under the NSF CREATE-IGERT training grant. We wish to thank Anny Chang, Jaclyn Chin, Ruiqin Pan, and Rongzhong Shao for their contributions in plasmid construction and crosses; Reinhard Fischer at the Karlsruhe Institute of Technology in Germany and Xin Xiang at the Uniformed Services University of the Health Sciences for sharing strains, and Roger Tsien at UC San Diego for providing the mCherry plasmid.

References

- Akhmanova, A., and Steinmetz, M.O. (2008) Tracking the ends: a dynamic protein network controls the fate of microtubule tips. *Nat Rev Mol Cell Biol* **9**: 309–322.
- Akhmanova, A., and Steinmetz, M.O. (2010) Microtubule +TIPs at a glance. *J Cell Sci* **123**: 3415–3419.
- Al-Bassam, J., Kim, H., Flor-Parra, I., Lal, N., Velji, H., and Chang, F. (2012) Fission yeast Alp14 is a dose-dependent plus end-tracking microtubule polymerase. *Mol Biol Cell* **23**: 2878–2890.

- Bieling, P., Laan, L., Schek, H., Munteanu, E.L., Sandblad, L., Dogterom, M., *et al.* (2007) Reconstitution of a microtubule plus-end tracking system *in vitro*. *Nature* **450**: 1100–1105.
- Bieling, P., Kandels-Lewis, S., Telley, I.A., van Dijk, J., Janke, C., and Surrey, T. (2008) CLIP-170 tracks growing microtubule ends by dynamically recognizing composite EB1/tubulin-binding sites. *J Cell Biol* **183**: 1223–1233.
- Blake-Hodek, K.A., Cassimeris, L., and Huffaker, T.C. (2010) Regulation of microtubule dynamics by Bim1 and Bik1, the budding yeast members of the EB1 and CLIP-170 families of plus-end tracking proteins. *Mol Biol Cell* **21**: 2013–2123.
- Busch, K.E., and Brunner, D. (2004) The microtubule plus end-tracking proteins mal3p and tip1p cooperate for cell-end targeting of interphase microtubules. *Curr Biol* **14**: 548–559.
- Carvalho, P., Gupta, M.L., Jr, Hoyt, M.A., and Pellman, D. (2004) Cell cycle control of kinesin-mediated transport of Bik1 (CLIP-170) regulates microtubule stability and dynein activation. *Dev Cell* **6**: 815–829.
- Currie, J.D., Stewman, S., Schimizzi, G., Slep, K.C., Ma, A., and Rogers, S.L. (2011) The microtubule lattice and plus-end association of *Drosophila* Mini spindles is spatially regulated to fine-tune microtubule dynamics. *Mol Biol Cell* **22**: 4343–4361.
- Dixit, R., Barnett, B., Lazarus, J.E., Tokito, M., Goldman, Y.E., and Holzbaur, E.L. (2009) Microtubule plus-end tracking by CLIP-170 requires EB1. *Proc Natl Acad Sci USA* **106**: 492–497.
- Efimov, V.P., Zhang, J., and Xiang, X. (2006) CLIP-170 homologue and NUDE play overlapping roles in NUDF localization in *Aspergillus nidulans*. *Mol Biol Cell* **17**: 2021–2034.
- Enke, C., Zekert, N., Veith, D., Schaaf, C., Konzack, S., and Fischer, R. (2007) *Aspergillus nidulans* Dis1/XMAP215 protein AlpA localizes to spindle pole bodies and microtubule plus ends and contributes to growth directionality. *Eukaryot Cell* **6**: 555–562.
- Fischer, R., Zekert, N., and Takeshita, N. (2008) Polarized growth in fungi – interplay between the cytoskeleton, positional markers and membrane domains. *Mol Microbiol* **68**: 813–826.
- Fridolfsson, H.N., and Starr, D.A. (2010) Kinesin-1 and dynein at the nuclear envelope mediate the bidirectional migrations of nuclei. *J Cell Biol* **191**: 115–128.
- Galjart, N. (2010) Plus-end-tracking proteins and their interactions at microtubule ends. *Curr Biol* **20**: R528–R537.
- Gouveia, S.M., and Akhmanova, A. (2010) Cell and molecular biology of microtubule plus end tracking proteins: end binding proteins and their partners. *Int Rev Cell Mol Biol* **285**: 1–74.
- Grallert, A., Beuter, C., Craven, R.A., Bagley, S., Wilks, D., Fleig, U., and Hagan, I.M. (2006) *S. pombe* CLASP needs dynein, not EB1 or CLIP170, to induce microtubule instability and slows polymerization rates at cell tips in a dynein-dependent manner. *Genes Dev* **20**: 2421–2436.
- Han, G.S., Liu, B., Zhang, J., Zuo, W.Q., Morris, N.R., and Xiang, X. (2001) The *Aspergillus* cytoplasmic dynein heavy chain and NUDF localize to microtubule ends and affect microtubule dynamics. *Curr Biol* **11**: 719–724.
- Harris, S.D., Read, N.D., Roberson, R.W., Shaw, B., Seiler, S., Plamann, M., and Momany, M. (2005) Polarisome meets Spitzenkörper: microscopy, genetics, and genomics converge. *Eukaryot Cell* **4**: 225–229.
- Higashitsuji, Y., Herrero, S., Takeshita, N., and Fischer, R. (2009) The cell end marker protein TeaC is involved in growth directionality and septation in *Aspergillus nidulans*. *Eukaryot Cell* **8**: 957–967.
- Horio, T. (2007) Role of microtubules in tip growth of fungi. *J Plant Res* **120**: 53–60.
- Horio, T., and Oakley, B.R. (2005) The role of microtubules in rapid hyphal tip growth of *Aspergillus nidulans*. *Mol Biol Cell* **16**: 918–926.
- Jiang, K., and Akhmanova, A. (2011) Microtubule tip-interacting proteins: a view from both ends. *Curr Opin Cell Biol* **23**: 94–101.
- Jiang, K., Toedt, G., Montenegro Gouveia, S., Davey, N.E., Hua, S., van der Vaart, B., *et al.* (2012) A Proteome-wide screen for mammalian SxIP motif-containing microtubule plus-end tracking proteins. *Curr Biol* **22**: 1800–1807.
- Kafer, E. (1977) Meiotic and mitotic recombination in *Aspergillus* and its chromosomal aberrations. *Adv Genet* **19**: 33–131.
- Kim, J.-M., Lu, L., Shao, R., Chin, J., and Liu, B. (2006) Isolation of mutations that bypass the requirement of the septation initiation network for septum formation and conidiation in *Aspergillus nidulans*. *Genetics* **173**: 685–696.
- Kim, J.-M., Zeng, C.T., Nayak, T., Shao, R., Huang, A., Oakley, B.R., and Liu, B. (2009) Timely septation requires SNAD-dependent spindle pole body localization of the septation initiation network components in the filamentous fungus *Aspergillus nidulans*. *Mol Biol Cell* **20**: 2874–2884.
- Kinoshita, K., Arnal, I., Desai, A., Drechsel, D.N., and Hyman, A.A. (2001) Reconstitution of physiological microtubule dynamics using purified components. *Science* **294**: 1340–1343.
- Komarova, Y., De Groot, C.O., Grigoriev, I., Gouveia, S.M., Munteanu, E.L., Schober, J.M., *et al.* (2009) Mammalian end binding proteins control persistent microtubule growth. *J Cell Biol* **184**: 691–706.
- Konzack, S., Rischitor, P.E., Enke, C., and Fischer, R. (2005) The role of the kinesin motor KipA in microtubule organization and polarized growth of *Aspergillus nidulans*. *Mol Biol Cell* **16**: 497–506.
- Lee, W.L., Oberle, J.R., and Cooper, J.A. (2003) The role of the lissencephaly protein Pac1 during nuclear migration in budding yeast. *J Cell Biol* **160**: 355–364.
- Li, W., Moriwaki, T., Tani, T., Watanabe, T., Kaibuchi, K., and Goshima, G. (2012) Reconstitution of dynamic microtubules with *Drosophila* XMAP215, EB1, and Sentin. *J Cell Biol* **199**: 849–862.
- Liu, B., and Morris, N.R. (2000) A spindle pole body-associated protein, SNAD, affects septation and conidiation in *Aspergillus nidulans*. *Mol Gen Genet* **263**: 375–387.
- Markus, S.M., Punch, J.J., and Lee, W.L. (2009) Motor- and tail-dependent targeting of dynein to microtubule plus ends and the cell cortex. *Curr Biol* **19**: 196–205.
- Mimori-Kiyosue, Y. (2011) Shaping microtubules into diverse patterns: molecular connections for setting up both ends. *Cytoskeleton* **68**: 603–618.
- Mourino-Perez, R.R., Linacre-Rojas, L.P., Roman-Gavilanes, A.I., Lew, T.K., Callejas-Negrete, O.A., Roberson, R.W.,

- and Freitag, M. (2013) MTB-3, a microtubule plus-end tracking protein (+TIP) of *Neurospora crassa*. *PLoS ONE* **8**: e70655.
- Muhua, L., Adames, N.R., Murphy, M.D., Shields, C.R., and Cooper, J.A. (1998) A cytokinesis checkpoint requiring the yeast homologue of an APC-binding protein. *Nat Rev Mol Cell Biol* **393**: 487–491.
- Nayak, T., Szewczyk, E., Oakley, C.E., Osmani, A., Ukil, L., Murray, S.L., et al. (2006) A versatile and efficient gene targeting system for *Aspergillus nidulans*. *Genetics* **172**: 1557–1566.
- Oakley, B.R., and Morris, N.R. (1980) Nuclear movement is β -tubulin dependent in *Aspergillus nidulans*. *Cell* **19**: 255–262.
- Oakley, B.R., and Morris, N.R. (1981) A β -tubulin mutation in *Aspergillus nidulans* that blocks microtubule function without blocking assembly. *Cell* **24**: 837–845.
- Osmani, S.A., May, G.S., and Morris, N.R. (1987) Regulation of the messenger RNA levels of *nimA*. A gene required for the G2-M transition in *Aspergillus nidulans*. *J Cell Biol* **104**: 1495–1504.
- Plamann, M., Minke, P.F., Tinsley, J.H., and Bruno, K.S. (1994) Cytoplasmic dynein and actin-related protein Arp1 are required for normal nuclear distribution in filamentous fungi. *J Cell Biol* **127**: 139–149.
- Riquelme, M., Fischer, R., and Bartnicki-Garcia, S. (2003) Apical growth and mitosis are independent processes in *Aspergillus nidulans*. *Protoplasma* **222**: 211–215.
- Rogers, S.L., Rogers, G.C., Sharp, D.J., and Vale, R.D. (2002) *Drosophila* EB1 is essential for proper assembly, dynamics, and positioning of the mitotic spindle. *J Cell Biol* **158**: 873–884.
- Sampson, K., and Heath, I.B. (2005) The dynamic behaviour of microtubules and their contributions to hyphal tip growth in *Aspergillus nidulans*. *Microbiology* **151**: 1543–1555.
- Schwartz, K., Richards, K., and Botstein, D. (1997) BIM1 encodes a microtubule-binding protein in yeast. *Mol Biol Cell* **8**: 2677–2691.
- Shaner, N.C., Campbell, R.E., Steinbach, P.A., Giepmans, B.N., Palmer, A.E., and Tsien, R.Y. (2004) Improved monomeric red, orange and yellow fluorescent proteins derived from *Discosoma* sp. red fluorescent protein. *Nat Biotechnol* **22**: 1567–1572.
- Sheeman, B., Carvalho, P., Sagot, I., Geiser, J., Kho, D., Hoyt, M.A., and Pellman, D. (2003) Determinants of *S. cerevisiae* dynein localization and activation: implications for the mechanism of spindle positioning. *Curr Biol* **13**: 364–372.
- Skube, S.B., Chaverri, J.M., and Goodson, H.V. (2010) Effect of GFP tags on the localization of EB1 and EB1 fragments *in vivo*. *Cytoskeleton* **67**: 1–12.
- Su, L.K., Burrell, M., Hill, D.E., Gyuris, J., Brent, R., Wiltshire, R., et al. (1995) APC binds to the novel protein EB1. *Cancer Res* **55**: 2972–2977.
- Szewczyk, E., Nayak, T., Oakley, C.E., Edgerton, H., Xiong, Y., Taheri-Talesh, N., et al. (2006) Fusion PCR and gene targeting in *Aspergillus nidulans*. *Nat Protoc* **1**: 3111–3120.
- Taheri-Talesh, N., Xiong, Y., and Oakley, B.R. (2012) The functions of myosin II and myosin V homologs in tip growth and septation in *Aspergillus nidulans*. *PLoS ONE* **7**: e31218.
- Takeshita, N., and Fischer, R. (2011) On the role of microtubules, cell end markers, and septal microtubule organizing centres on site selection for polar growth in *Aspergillus nidulans*. *Fungal Biol* **115**: 506–517.
- Takeshita, N., Mania, D., Herrero, S., Ishitsuka, Y., Nienhaus, G.U., Podolski, M., et al. (2013) The cell-end marker TeaA and the microtubule polymerase AlpA contribute to microtubule guidance at the hyphal tip cortex of *Aspergillus nidulans* to provide polarity maintenance. *J Cell Sci* **126**: 5400–5411.
- Tirnauer, J.S., and Bierer, B.E. (2000) EB1 proteins regulate microtubule dynamics, cell polarity, and chromosome stability. *J Cell Biol* **149**: 761–766.
- Tirnauer, J.S., O'Toole, E., Berrueta, L., Bierer, B., and Pellman, D. (1999) Yeast Bim1p promotes the G1-specific dynamics of microtubules. *J Cell Biol* **145**: 993–1007.
- Tirnauer, J.S., Grego, S., Salmon, E.D., and Mitchison, T.J. (2002) EB1-microtubule interactions in *Xenopus* egg extracts: role of EB1 in microtubule stabilization and mechanisms of targeting to microtubules. *Mol Biol Cell* **13**: 3614–3626.
- Tsai, J.W., Lian, W.N., Kemal, S., Kriegstein, A.R., and Vallee, R.B. (2010) Kinesin 3 and cytoplasmic dynein mediate interkinetic nuclear migration in neural stem cells. *Nat Neurosci* **13**: 1463–1471.
- Vaughan, K.T., Tynan, S.H., Faulkner, N.E., Echeverri, C.J., and Vallee, R.B. (1999) Colocalization of cytoplasmic dynein with dynactin and CLIP-170 at microtubule distal ends. *J Cell Sci* **112**: 1437–1447.
- Vitre, B., Coquelle, F.M., Heichette, C., Garnier, C., Chretien, D., and Arnal, I. (2008) EB1 regulates microtubule dynamics and tubulin sheet closure *in vitro*. *Nat Cell Biol* **10**: 415–421.
- Xiang, X., and Oakley, B.R. (2010) The cytoskeleton in filamentous fungi. In *Cellular and Molecular Biology of Filamentous Fungi*. Borkovich, K., and Ebbole, D. (eds). Washington, DC: ASM Press, pp. 209–223.
- Xiang, X., Beckwith, S.M., and Morris, N.R. (1994) Cytoplasmic dynein is involved in nuclear migration in *Aspergillus nidulans*. *Proc Natl Acad Sci USA* **91**: 2100–2104.
- Xiang, X., Roghi, C., and Morris, N.R. (1995) Characterization and localization of the cytoplasmic dynein heavy chain in *Aspergillus nidulans*. *Proc Natl Acad Sci USA* **92**: 9890–9894.
- Xiang, X., Han, G.S., Winkelmann, D.A., Zuo, W.Q., and Morris, N.R. (2000) Dynamics of cytoplasmic dynein in living cells and the effect of a mutation in the dynactin complex actin-related protein Arp1. *Curr Biol* **10**: 603–606.
- Yu, K.L., Keijzer, N., Hoogenraad, C.C., and Akhmanova, A. (2011) Isolation of novel +TIPs and their binding partners using affinity purification techniques. *Methods Mol Biol* **777**: 293–316.
- Zanic, M., Widlund, P.O., Hyman, A.A., and Howard, J. (2013) Synergy between XMAP215 and EB1 increases microtubule growth rates to physiological levels. *Nat Cell Biol* **15**: 688–693.
- Zhang, J., Li, S., Fischer, R., and Xiang, X. (2003) Accumulation of cytoplasmic dynein and dynactin at microtubule plus ends in *Aspergillus nidulans* is kinesin dependent. *Mol Biol Cell* **14**: 1479–1488.

Zhang, J., Zhuang, L., Lee, Y., Abenza, J.F., Peñalva, M.A., and Xiang, X. (2010) The microtubule plus-end localization of *Aspergillus* dynein is important for dynein-early-endosome interaction but not for dynein ATPase activation. *J Cell Sci* **123**: 3596–3604.

Zhang, J., Tan, K., Wu, X., Chen, G., Sun, J., Reck-Peterson, S.L., *et al.* (2011) *Aspergillus* myosin-V supports polarized

growth in the absence of microtubule-based transport. *PLoS ONE* **6**: e28575.

Supporting information

Additional supporting information may be found in the online version of this article at the publisher's web-site.